Robust Mission Planning of UAV Networks for Environmental Sensing

Ahmed Boubrima and Edward W. Knightly
Rice University, Houston, Texas
{ahmed.boubrima,knightly}@rice.edu

Abstract

In this paper, we first investigate the quality of aerial air pollution measurements and characterize the main error sources of drone-mounted gas sensors. To that end, we build ASTRO+, an aerial-ground pollution monitoring platform, and use it to collect a comprehensive dataset of both aerial and reference air pollution measurements. We show that the dynamic airflow caused by drones affects temperature and humidity levels of the ambient air, which then affect the measurement quality of gas sensors. Then, in the second part of this paper, we leverage the effects of weather conditions on pollution measurements' quality in order to design a UAV mission planning algorithm that adapts the trajectory of the drones while taking into account the quality of aerial measurements. We evaluate our mission planning approach based on a VOC pollution dataset and show a high performance improvement that is due to the fine characterization of the measurement errors.

CCS Concepts

• **Computer systems organization** → *Embedded and cyber physical systems*; • **Networks** → *Network algorithms.*

1 Introduction

Unmanned aerial vehicles (UAVs), commonly known as drones, are used in many environmental applications and especially air pollution monitoring, which requires high spatial resolution sensing [13]. Indeed, whether the objective is to perform a full mapping of pollution concentrations or to characterize a specific pollution plume in case of a gas leak, drones offer better spatial resolution compared to static and car-mounted sensing solutions [1]. However, due to their power constraints, drones are limited in terms of sensing resources and require efficient mission planning in order to perform measurements at the most informative sensing locations within their restricted flight time [4]. The performance of UAV mission planning algorithms highly depends on the quality of aerial sensing since low quality measurements may lead to poor predictions of the most informative sensing locations [7].

Evaluation of pollution aerial measurements' quality. In this paper, we first investigate the quality of aerial measurements of air pollution and characterize the main error sources of drone-mounted gas sensors. Although the quality of aerial pollution measurements has been studied previously [5, 15], such work provides only a qualitative evaluation and do not quantify the amount of error that is due to the main error sources, which are identified to be mainly caused by the airflow generated from the drones' propellers and the vibrations of the drones. In contrast, we conduct a comprehensive measurement campaign of both aerial and ground data in order to quantify the multi-factor non-homogeneous pollution sensing errors. We show that the dynamic airflow caused by drones affects first temperature and humidity levels of the ambient air, which then affect the measurement quality of gas sensors.

Without loss of generality, we focus on measuring Volatile Organic Compound (VOC) pollutants, which provide a strong signature of both industrial and traffic emissions. We build *ASTRO+*, which is an aerial-ground air pollution monitoring platform where ground sensors provide reference measurements and drones are equipped with temperature, humidity and wind velocity sensors in addition to light-weight pollution sensors. We collect a comprehensive dataset of both aerial and ground measurements and use it to characterize the impact of weather conditions on the quality of drone-mounted pollution sensors. We show that VOC aerial measurements can be inferred with up to 88% accuracy based on humidity and temperature levels of the ambient air.

Robust UAV mission planning. In the second part of this paper, we leverage these discovered effects of weather conditions on pollution measurements' quality in order to design a UAV mission planning algorithm that adapts the trajectory of the drones while taking into account the quality of aerial measurements that is inferred from weather conditions. Compared to most existing work [2, 8, 17–19], we consider the dynamic nature of aerial sensing errors and do not rely on static error values that are provided by manufacturers.

After a training phase prior to the flight mission in order to characterize the impact of temperature, humidity and wind velocity on aerial measurements of pollution concentrations, our mission planning approach operates in 2 phases: UAVs are first sent to uniformly distributed locations in order to learn the spatial correlations of air pollution concentrations; Then in the second phase, these spatial correlations are used together with the inferred aerial measurements' quality in order to optimize the subsequent measurement locations of the drones. We evaluate our optimization approach based on our dataset of VOC measurements and show a high performance improvement that is due to the fine characterization of the measurement errors.

DroNet'20, June 19, 2020, Toronto, ON, Canada

ACM ISBN 978-1-4503-8010-2/20/06…$15.00
https://doi.org/10.1145/3396864.3399698

Related work

Characterization of the quality of pollution aerial measurements. Due to the non-instantaneous response time of pollution sensors, rotatory wing UAVs are preferred over fixed wing drones when performing air pollution data collection. However, when propellers are spinning, air pollution measurements are affected and their errors need to be properly characterized. Existing work focuses mainly on the qualitative evaluation of these errors. For instance, some prior work performs multiple experimental flights in an urban area and then correlates drone measurements with the proximity to traffic sources [5]. This work showed the high noise level in pollution measurements and the need of a proper characterization of measurement errors. Other prior work proposes to characterize the airflow generated by the propellers of the drones and use the wind velocity level as a qualitative indicator of pollution measurements' errors [10, 12, 15]. In contrast, we infer the measurements' errors by co-locating drones and ground sensors and then extracting the correlations between pollution data and wind in addition to temperature and humidity.

UAV mission planning for environmental mapping. Mobile sensors' mission planning for environmental monitoring in general and air pollution mapping in particular has been extensively studied in the literature [2, 8, 17–19]. Most existing work relies on the spatial correlation of air pollution concentrations: that is, closer locations have higher probability of being at the same concentration level [3]. Based on that, the uncertainty of pollution estimation at unmeasured locations is formulated as a function of the spatial correlations of the measurements. The optimized sensing mission plan (i.e. the optimal set of sensing way-points) is then obtained by minimizing the uncertainty of pollution estimations at unmeasured locations. In contrast, we propose to couple the pollution spatial correlations with a fine characterization of aerial measurements' quality in the optimization process of UAV mission planning.

2 ASTRO+: Aerial-Ground air pollution monitoring platform

2.1 Overview

ASTRO+ is an environmental sensing platform that includes two main sensing technologies: ground reference sensors and aerial sensing using drones. We focus on measuring Volatile Organic Compounds (VOCs), which provide a good signature of both traffic and industry related air pollution. For reference ground sensing, we selected Defiant's FROG-5000, which uses gas chromatography to measure the 4 major VOC pollutants (Benzene, Toluene, Ethylbenzene and Xylene) at the ppb level. Because reference measurement sensors like the FROG-4000 are heavy and cannot be deployed easily on drones, we use Photo Ionization Detection (PID) VOC sensors for aerial measurements. PID sensors can weigh as little as $100g$ and provide fast response measurements compared to other light-weight sensing solutions such as electrochemical sensors. After careful analysis of existing PID sensors, we selected ION Science's miniPID2 VOC sensor, which has limited temperature and humidity effects compared to other sensors in the market.

2.2 Architecture of ASTRO+

ASTRO+ includes 3 layers: sensing, data storage and a third layer for data visualization and user notification. Data that is collected by both drones (PID sensors) and ground sensors (Gas chromatography in addition to PID) is sent over WiFi to an Internet-hosted database. The database is connected to a mobile app and a web service that allow community users to visualize both real-time measurements and historical data. In addition to raw measurements of both ground sensors and last drone missions, the mobile app also indicates the air quality based on EPA's air pollution thresholds. In addition to data visualization, users can subscribe to SMS and E-mail notifications in order to be informed in real-time about pollution peak levels.

2.3 UAV system

We build our UAV-based sensing system as an extension of our *ASTRO* platform [11]. *ASTRO* is a UAV network platform that is *Autonomous* and *Tetherless* in the sense that drones form an infrastructureless wireless network and don't need a base station to make their sensing decisions. Thanks to using carbon fiber light-weight frames, *ASTRO* drones allow up to 15min flight time and up to 1.5kg of payload. *ASTRO* also uses hardware components that are widely used within the open-source community, namely the *Pixhawk* flight controller to manage the avionics part and the *Raspberry Pi* as a companion computer in order to manage the network communication part.

We extend *ASTRO* by deploying lightweight VOC, temperature, humidity and wind sensors while offering low-noise measurements. This is achieved by first locating the sensors right next to the center of the drone in order to minimize turbulence effects that are caused by the propellers [15]. In addition to that, we isolate the power source of the environmental sensors from the flight controller and companion computer battery in order to maintain the stability of the input voltage of the sensors. Drone measurements are performed once per second. In terms of resolution, temperature values are reported within $\pm 1^{\circ}$ Celsius, relative humidity is reported within $\pm 1\%$ and VOC measurements are reported at the ppb level.

3 Evaluation of aerial sensing errors

In this section, we use the aerial and reference ground sensors of *ASTRO+* to analyze the quality of aerial measurements of VOCs. Prior work suggested that the dynamic airflow created by drones' propellers and drone vibrations affects the quality of the measurements. However, it is not previously known how these dynamics affect the sensing mechanism of drone-mounted pollution sensors. Indeed, the main light-weight gas sensing technologies (photo-ionization-based and electrochemical sensors) can be easily affected by changes in weather conditions such as temperature and humidity but not necessarily the airflow and wind velocity [9]. In this section, we propose a fine characterization of these effects using an experimentally collected dataset.

3.1 Experimental scenario

We performed multiple data collection experiments in Milby Park (Houston, Texas), a residential neighborhood that is highly exposed to both traffic pollution (facing a highway) and industrial pollution (located within less than 2 miles of 3 chemical plants). We collected in different locations and times during *February 2020* more than $1,000$ measurements of both ground reference data and aerial data of VOC pollution concentrations in addition to aerial data of temperature, relative humidity and wind velocity. Each measurement was performed while having the drone hovering at about 2.5m and located within 4 to 5 meters of the ground sensor, which was sampling at an altitude close the one of the drone (1.5m). In order to reduce sensing errors during the measurement campaign, and as recommended by the manufacturer, both aerial and ground sensors were properly calibrated in the field against reference gas concentrations of Isobutylene (a VOC gas that is commonly used to calibrate PID sensors).

3.2 Evaluation results

Fig. 1 depicts the obtained VOC ground measurements on the x-axis and the corresponding aerial measurements on the y-axis. Note that even though aerial measurements may underestimate the real concentrations in some few cases going down to as low as 20*ppb* compared to the lowest reference concentration of 40*ppb*, the overall bias of drone data is very low and does not exceed 1*ppb* thanks to the proper calibration of the sensors prior to the measurement campaign. However, the overall standard deviation of aerial sensing errors is substantial and exceeds 6% of the full range of the measured concentrations (96*ppb*). This is clearly due to the dynamic nature of aerial measurements where drone vibrations and hence propellers' effects are very variable and therefore difficult to predict.

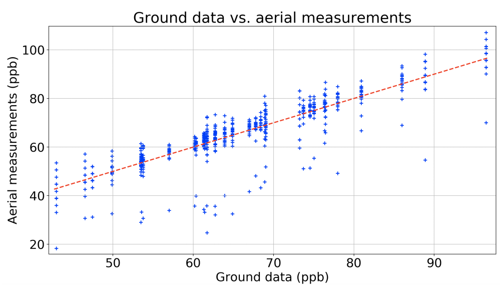

Figure 1: Ground measurements vs. aerial measurements.

In order to characterize the main sources of aerial measurement errors, we depict in Fig. 2 the standard deviation of the error of aerial measurements with respect to ground reference data depending, respectively, on wind velocity (generated by the drone propellers), temperature, relative humidity and absolute humidity.

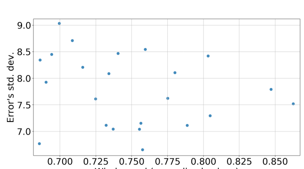

(a) Effects of wind velocity

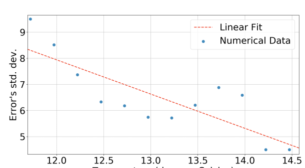

(b) Effects of temperature

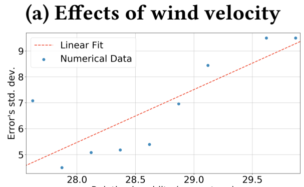

(c) Effects of relative humidity

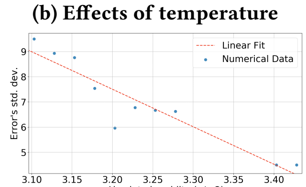

(d) Effects of absolute humidity

Figure 2: Effects of wind, temperature and humidity on the quality of VOC aerial measurements.

The air flow speed generated by the propellers seems to have a very poor correlation, which does not exceed 25%. However, temperature and relative humidity dynamics (caused in part by the airflow dynamics that are due to propellers) correlate with aerial measurements' quality better than wind and yield more than 60% of linear correlation and more than 90% of polynomial 3rd order correlation. This is mainly due to the high sensitivity of pollution sensors in general to temperature [9], and also the sensitivity of PID sensors in particular to the level of water vapor in the air [14]. This is why water vapor (also defined as absolute humidity and calculated based on both temperature and relative humidity) provides almost 90% correlation with aerial measurements quality when using just the 1st order polynomial fit. We show in the next section that this linear fit could be used to improve the quality of aerial measurements during environmental mapping missions.

Discussion: The results presented in this section show that co-locating temperature, humidity and wind sensors with air pollution sensors could help infer the quality of pollution aerial measurements subject to a proper training prior to environmental mapping missions. For instance, and as shown in this section, PID measurements' quality could be inferred to almost 90% using absolute humidity data (calculated based on temperature and relative humidity measurements). For other pollution sensors (electrochemical sensors for instance), the predictive variables could be different than absolute humidity or a combination of multiple weather conditions but the correlation should still remain high as most air pollution sensors are very sensitive to weather conditions [9]. This measurements' quality inference fact could then be used to characterize pollution aerial sensing quality at future measurement locations by first interpolating the already collected weather data and then using the results of this interpolation to predict pollution measurements' quality at future sensing points.

4 Robust mission planning for air pollution mapping

4.1 Overview

The experimental study presented in the previous section confirms that pollution aerial measurements' quality is dynamic and non homogeneous with respect to the measurement context (temperature, humidity and wind levels of the ambient air). These dynamics should have a direct impact on the performance of UAV mission planning algorithms since low quality measurements may lead to a bad estimation of the drones' mission plans. Based on that fact, we design in this section a UAV mission planning approach while relying on a fine characterization of aerial measurements' quality in addition to the inherent pollution spatial correlations. Given an input region to be monitored and a set of pollution-sensing UAVs with limited flight time, we aim at: i) determining a selection of points that should be sampled by the UAV network so that the obtained measurements yield a low-error estimated pollution map; and ii) determining for each UAV the locations that should be visited so that the covered points of interest are visited by at least one drone. Here, the estimated pollution map is obtained by interpolating the data collected at the optimal measurement locations.

The proposed mission planning approach operates as follows: after a training phase prior to the flight mission in order to quantify the impact of temperature, humidity and wind velocity on aerial measurements of pollution concentrations, UAVs are first sent to uniformly distributed locations in order to characterize the spatial correlations of air pollution concentrations. Then, these spatial correlations are used together with the inferred aerial measurements' quality in order to optimize the following measurement locations of the drones. The optimal measurement locations of each drone are obtained by minimizing the overall variance of the interpolated concentrations' errors while taking into account the aerial sensing constraints (the dynamic sensing error and the response time of pollution sensors, the speed of the drone and the drone's battery capacity).

4.2 Air pollution mapping

Before getting into the details of our UAV mission planning process, we first present the mathematical formulation that allows us to estimate pollution concentrations at unmeasured locations given a set of space locations with a limited number of measurements. We focus on the optimal linear interpolation method, which is the most used air pollution data interpolation technique in the literature [16]. Without loss of generality, and due to the relatively short flight time of drones, we focus on the case of pollution concentrations that change only in space and not in time.

Let $\boldsymbol{p}$ be a vector of l discrete points approximating the space in 2D or 3D. **i.e.** $\boldsymbol{p} = [p_1, p_2, ..., p_l]^T$ where $p_i = (x_i, y_i, z_i)$. We use $\mathbf{g} \in \mathbb{R}^l$ to denote the unknown ground truth timely-static pollution concentrations at the l points of space. **i.e.** $\mathbf{g} = [g_1, g_2, ..., g_l]^T$ where g_i is the pollution concentration at point i. Let $\boldsymbol{z} \in \mathbb{R}^n$ be a set of measurements performed at n different locations in space $\boldsymbol{p}$. **i.e.** $\boldsymbol{z} = [z_1, z_2, ..., z_n]^T$ where z_i is measurement number i. In order to map measurements to space locations, we define a matrix $H \in \mathbb{R}^{n \times l}$ where each matrix element h_{ij} is a Boolean set to 1 if measurement number i is performed at point j. Let θ_i be the error of measurement z_i with respect to ground truth g_i. We denote the variance of sensing error θ_i using r_i, which can be inferred based on co-located measurements of temperature, humidity and wind velocity as demonstrated in the previous section of this paper. In addition, we assume that θ_i has a zero mean as this is usually the case when pollution sensors are properly calibrated. We also assume that pollution measurement errors are uncorrelated because they mainly depend on the electronics of the sensing mechanism. Hence, the covariance matrix of sensing errors, $R \in \mathbb{R}^{n \times n}$, is a diagonal matrix.

Air pollution concentrations g_i are inherently correlated in space [16]. We denote the spatial correlation matrix of pollution concentrations by $B \in \mathbb{R}^{l \times l}$. Each matrix element b_{ij} reflects for space locations i and j the probability of being at the same concentration level.

Using the measurement vector $\boldsymbol{z}$ and the matrix H defining measurement locations, our objective is to obtain an estimation vector $\boldsymbol{c} \in \mathbb{R}^l$ by interpolating pollution concentrations at unmeasured locations. In the case of optimal linear interpolation [6], $\boldsymbol{c}$ is defined in matrix form as

$$\boldsymbol{c} = W\boldsymbol{z}$$

such that $\boldsymbol{c}$ is a linear combination of the collected measurements. The interpolation weights are defined by the matrix W, which is calculated as in [6]

$$W = BH^T(R + HBH^T)^{-1} \tag{1}$$

and is a function of sensing quality defined by matrix R in addition to the spatial correlation matrix of pollution concentrations B. Let η_i denote the interpolated concentrations' errors with respect to the unknown ground truth value at each point i (i.e. $\boldsymbol{\eta} = \boldsymbol{c} - \boldsymbol{g}$). The covariance matrix of $\boldsymbol{\eta}$ (denoted F) is calculated as in [6]

$$F = (I_l - BH^T(R + HBH^T)^{-1}H)B, \tag{2}$$

where I_l is the identity matrix. Based on F, we define the overall mapping error of a given interpolated map $\boldsymbol{c}$ corresponding to a given measurements' vector $\boldsymbol{z}$ as

$$\sum_{i \in [1,l]} c_i^{\alpha} \times f_{ii},$$

where α is a parameter used to emphasize the interpolation error at polluted locations compared to the slightly polluted ones.

4.3 Mission planning process

We consider a mobile sensing system consisting of m drones that are equipped with air pollution sensors which are used to collect measurements $\boldsymbol{z}$ within the monitoring region $\boldsymbol{p}$. In order to quantify the covariance matrix of pollution measurements' errors R, drones are also equipped with temperature, humidity and wind sensors. This allows us to infer on-the-fly r_i, the error variance of each already collected measurement z_i in addition to inferring the measurement error variance at future mission locations by interpolating the already collected temperature, humidity and wind data. The measurement error inference is obtained based on a training phase that is performed prior to the pollution mapping mission by co-locating drones and reference sensors as shown in Section 3.

Because of the response time of pollution sensors, drones need to hover for a time $\mathcal{T}_{hover}$ in order to obtain a pollution measurement at a given space point [9]. In addition to the hover time constraint, we assume that drones travel at a constant speed v. Based on that, we calculate the travel times between each pair of points (i, j) that we denote by $\mathcal{T}_{travel}(i, j)$. In addition, let $\mathcal{T}_{flight}$ be the maximum flight time of each drone, which mainly depends on the weight of the drone, the capacity of the battery and the drone speed v.

In terms of communication, we assume that drones remain connected to the base station when travelling within the monitoring region $\boldsymbol{p}$. This is usually the case in urban environments and industrial areas. In addition, we assume that the communication delay between the drones and the base station is minimal compared to the measurement hover time of the drones, which could be as high as $30s$ [9].

Our mission planning approach operates in two phases: a learning phase and an optimization phase. The objective of the first phase is to learn the spatial correlation matrix of pollution concentrations B. In the second phase, we define and solve an optimization model while relying on spatial correlations B and non-homogeneous measurements' quality R in order to guide the drones to the locations that allow us to get a vector $\boldsymbol{c}$ of estimated concentrations with a corresponding covariance matrix F where the mapping quality defined in the previous section ($\sum_{i \in [1,l]} c_i^{\alpha} \times f_{ii}$) is minimized.

Phase 1: Initialization phase. Our objective in phase 1 is to characterize the spatial correlations of pollution concentrations by estimating the matrix B. To that end, we perform n_0 measurements that are uniformly distributed in the monitoring region. We first divide the monitoring region into m sub-regions having the same surface area. Each drone is then sent to one of these sub-regions and performs n_0/m uniformly distributed measurements. Note that n_0 is a parameter that should be chosen carefully depending on the size of the monitoring region. At the end of phase 1, the obtained pollution measurements, denoted by $\boldsymbol{z^0}$, in addition to the inferred measurements' quality matrix R, are sent over to the base station. Based on that data, the base station performs the characterization of the spatial correlations as explained later in Section 4.4 and mission planning decisions as explained in Section 4.5.

Phase 2: Optimization phase. Our objective in phase 2 is to use the obtained B matrix in order to find the best way-points where drones should perform their measurements while taking into account flight time constraints. The optimization algorithm is run at the base station at the end of the initialization phase. As a result, each drone gets the optimal mission plan with respect to the current characterization of pollution spatial correlations. Each drone follows then the provided mission plan and each performed measurement is sent right away to the base station. The latter uses the new data in order to refine the characterization of pollution spatial correlations at a specific rate. The new characterization of spatial correlations is then used to refine the optimal mission plans of the drones and this process continues until no more data could be performed. At the end, the base station uses the full set of the obtained measurements combined with the inferred sensing quality and the final characterization of pollution spatial correlations in order to calculate the final interpolated concentrations $\boldsymbol{c}$.

4.4 Robust spatial correlation characterization

Given a set of already collected measurements $\boldsymbol{z^0} \in \mathbb{R}^{n_0}$ in addition to online inferred measurements' quality R, our aim is to estimate the pollution spatial correlations B. We recall that each matrix element b_{ij} corresponds to the correlation between the *unknown* ground truth concentrations g_i and g_j. In order to estimate the pollution spatial correlation between each pair of locations i and j, we first define as $D(i,j)$ the set of sampled location pairs that are within a Euclidean distance close to the distance between locations i and j. Mathematically, the set $D(i,j)$ can be written as

$$D(i,j) = \{(a,b) \mid z_a, z_b \in \boldsymbol{z}^0 \ \ \& \ \ \|p_a - p_b\| = \|p_i - p_j\| \pm \Delta\}.$$

Based on $D(i,j)$, we estimate the b_{ij} spatial correlation as

$$b_{ij} = corr\left(\begin{bmatrix} \frac{z_{a_1}}{r_{a_1}+r_{b_1}} \\ \vdots \\ \frac{z_{a_{|D|}}}{r_{a_{|D|}}+r_{b_{|D|}}} \end{bmatrix}, \begin{bmatrix} \frac{z_{b_1}}{r_{a_1}+r_{b_1}} \\ \vdots \\ \frac{z_{b_{|D|}}}{r_{a_{|D|}}+r_{b_{|D|}}} \end{bmatrix}\right) \tag{3}$$

This provides a robust estimation of $corr(g_i, g_j)$ while taking into account measurement errors by normalizing the measurements within each pair of points (a,b) using their respective error's variance r_a and r_b. The outcome of this normalization process is that low-quality measurements (**i.e.,** pairs (a,b) where either r_a or r_b is high) become less involved in the final estimated correlations b_{ij} whereas high-quality measurements (**i.e.,** pairs (a,b) where both r_a and r_b are low) are emphasized.

4.5 Robust mission planning optimization

Using the obtained characterization of spatial correlations B and the inferred measurements quality matrix R, our objective is to find the best locations that offer the best interpolation of pollution concentrations. In addition, we ensure that the selected locations can be sampled with the m drones subject to their remaining flight time $\mathcal{T}_{flight}$. We determine for each drone the best ordered set of sampling points by solving the following optimization model:

$$\begin{aligned} &\textbf{Minimize} \quad \sum_{i\in[1,l]} c_i^{\alpha} \times f_{ii} \\ &\textbf{Subject to} \quad \text{Eq.}(1),\ \text{Eq.}(2) \text{ and flight constraints} \end{aligned}$$

The objective function ensures the minimization of the overall variance of estimated concentration errors $f_{ii},\ i \in [1,l]$ while emphasizing the interpolation error at polluted locations compared to the slightly polluted ones. The minimization of the interpolation error's variance is performed with respect to the matrix H, which is the main decision variable in the optimization process and defines the best aerial sensing locations. In order to take into account the aerial sensing requirements, we constrain the sensing locations so that they are ordered in a way that takes into account the necessary sampling hover time in addition to drone travel times when moving from one location to another.

We solve our mission planning optimization model using commercial optimization solvers (IBM CPLEX) in the case of small monitoring regions. In order to scale our approach to large regions, we propose to solve the optimization model to get only a partial mission plan for each drone and then update the mission plans as the drones are flying.

4.6 Experimental evaluation

Dataset: We evaluate our mission planning approach using a set of 30 pollution maps of aerial and ground measurements of VOC pollutants collected in February 2020 using our sensing platform *ASTRO+*. We also use as input the collected absolute humidity maps in order to infer online VOC sensing errors since absolute humidity is highly correlated with aerial measurements' quality as shown in section 3. Each collected data map corresponds to a grid of 34 data points ($l = 34$) within the Milby Park residential neighborhood (Houston, Texas).

Flight constraints: We assume that drones fly high enough to avoid obstacles and that their flight speed is fixed at $2m/s$ for safety reasons. We set the hover time of each drone to $10s$ since we are focusing on VOC sensors, which have an acceptable response time that is usually within few seconds. We consider flight times of up to 30min where the first 10min are reserved to the initialization phase of our mission planning approach. This allows us to perform 6 uniformly distributed initial measurements ($n_0 = 6$), which is necessary for an initial characterization of pollution spatial correlations matrix B.

Performance metric: We simulate our mission planning approach while using the aerial data maps each time a drone sample is performed. Then we evaluate the quality of the output of each simulation by comparing the final interpolated map of aerial data to the corresponding reference ground map. We use the relative RMSE as a performance metric to evaluate the percentage of interpolation error of each environmental sensing mission.

Performance benchmarks: We compare the results of our robust mission planning to the following baselines:

- *Omniscient planning:* this is the best mission planning that could be obtained while relying on the real drift of aerial measurements (assumed to be hypothetically known). Given a number of sampling locations to optimize, we perform an exhaustive search to find the best combination of measurement locations that minimize the RMSE evaluation metric.

- *Traditional mission planning:* in this case, measurement error variance is assumed homogeneous and provided by the manufacturer as in most prior work. To evaluate this case, we simulate our optimization approach while setting the measurement error's variance r_i of each point i to 36 ppb^2 , which is the overall sensing errors' variance obtained in our VOC dataset.
- *Random uniform:* this corresponds to flying the drone to random sensing locations following the uniform distribution.

Evaluation results

Fig. 3 depicts the results obtained while considering a single drone with an overall flight time of up to 30min, which allows the drone to sample on average up to 15 locations including the measurements collected during the 10min of the initialization phase.

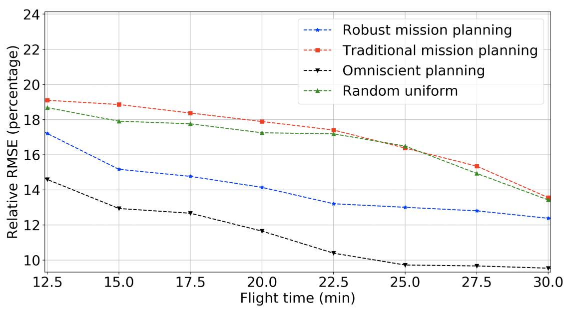

Figure 3: Environmental mapping performance evaluation.

The results show that due to the dynamic and non homogeneous nature of aerial sensing quality, traditional mission planning fails to send the drones to the most informative locations and selects instead measurement locations that are almost uniformly distributed in the monitoring region. This is due to the optimization objective function of traditional mission planning which only depends on spatial correlations since the variance of sensing errors is assumed homogeneous. Compared to that, and due to taking into account the heterogeneous nature of aerial sensing errors, our approach adjusts the spatial density of selected measurement locations depending on the sensing quality. This helps first better characterize the spatial correlations of pollution concentrations and then improve the interpolation performance by using the most accurate aerial data. As a result, our robust mission planning outperforms traditional solutions by up to $2.5x$ improvement factor (calculated with respect to the omniscient planning).

Note that our performance improvement decreases as the drone's flight time is extended. This is due to the small size of the monitoring region (500m x 500m), where a 30min flight time allows a single drone to sample almost half of the grid points and as a result obtain good interpolation quality even with uniformly distributed measurement locations. However, our approach, being efficient even with limited sensing resources, allows us to monitor large deployment regions especially when high flight speeds are allowed.

5 Conclusion

In this paper, we propose a robust mission planning approach that adapts the trajectory of the drones while taking into account the quality of aerial measurements that is inferred from weather conditions. Compared to existing mission planning algorithms, we propose in our work to couple the pollution spatial correlations with a fine characterization of aerial measurements' quality in the optimization process of UAV mission planning. We evaluate our mission planning approach based on our dataset of VOC measurements and show a high-performance improvement that is due to the fine characterization of the measurement errors.

Acknowledgments

This research was supported by Cisco, Intel, and by NSF grant CNS-1801865. We thank the interns of the ASTRO team for their help with the experiments.

References

[1] A. Anjomshoaa, F. Duarte, D. Rennings, T. J Matarazzo, P. deSouza, and C. Ratti. 2018. City scanner: Building and scheduling a mobile sensing platform for smart city services. *IEEE Internet of Things Journal* 5, 6 (2018), 4567–4579.

[2] A. Belkhiri, W. Bechkit, and H. Rivano. 2018. Virtual Forces based UAV Fleet Mobility Models for Air Pollution Monitoring. In *2018 IEEE 43rd Conference on Local Computer Networks (LCN)*. IEEE, 481–484.

[3] A. Boubrima, W. Bechkit, and H. Rivano. 2019. On the Deployment of Wireless Sensor Networks for Air Quality Mapping: Optimization Models and Algorithms. *IEEE/ACM Transactions on Networking* 27, 4 (2019), 1629–1642.

[4] T. Cabreira, L. Brisolara, and P. R Ferreira. 2019. Survey on Coverage Path Planning with Unmanned Aerial Vehicles. *Drones* 3, 1 (2019), 4.

[5] Q. Gu, D. R Michanowicz, and C. Jia. 2018. Developing a modular unmanned aerial vehicle (UAV) platform for air pollution profiling. *Sensors* 18, 12 (2018), 4363.

[6] E. Kalnay. 2003. *Atmospheric modeling, data assimilation and predictability.* Cambridge university press.

[7] R. Khodayi-mehr, W. Aquino, and M. Zavlanos. 2019. Model-based active source identification in complex environments. *IEEE Transactions on Robotics* 35, 3 (2019), 633–652.

[8] A. Krause, C. Guestrin, A. Gupta, and J. Kleinberg. 2011. Robust sensor placements at informative and communication-efficient locations. *ACM Transactions on Sensor Networks (TOSN)* 7, 4 (2011), 31.

[9] MI Mead, OAM Popoola, GB Stewart, P Landshoff, M Calleja, M Hayes, JJ Baldovi, MW McLeod, TF Hodgson, and J Dicks. 2013. The use of electrochemical sensors for monitoring urban air quality in low-cost, high-density networks. *Atmospheric Environment* 70 (2013), 186–203.

[10] P. Neumann. 2013. Gas source localization and gas distribution mapping with a micro-drone. (2013).

[11] R. Petrolo, Y. Lin, and E. Knightly. 2018. ASTRO: Autonomous, Sensing, and Tetherless netwoRked drOnes. In *Proceedings of the 4th ACM Workshop on Micro Aerial Vehicle Networks, Systems, and Applications*. 1–6.

[12] JJ Roldán, G. Joossen, D. Sanz, J. Del Cerro, and A. Barrientos. 2015. Mini-UAV based sensory system for measuring environmental variables in greenhouses. *Sensors* 15, 2 (2015), 3334–3350.

[13] H. Shakhatreh, A. Sawalmeh, A. Al-Fuqaha, Z. Dou, E. Almaita, I. Khalil, N.S. Othman, A. Khreishah, and M. Guizani. 2019. Unmanned aerial vehicles (UAVs): A survey on civil applications and key research challenges. *IEEE Access* 7 (2019), 48572–48634.

[14] Rae Systems. 2013. The PID Handbook: Theory and Applications of Direct-Reading Photoionization Detectors (PIDs).

[15] T.F. Villa, F. Salimi, K. Morton, L. Morawska, and F. Gonzalez. 2016. Development and validation of a UAV based system for air pollution measurements. *Sensors* 16, 12 (2016), 2202.

[16] D. Wong, L. Yuan, and S. Perlin. 2004. Comparison of spatial interpolation methods for the estimation of air quality data. *Journal of Exposure Science and Environmental Epidemiology* 14, 5 (2004), 404–415.

[17] Y. Xiang, L. Bai, R. Pledrahita, R. Dick, Q. Lv, M. Hannigan, and L. Shang. 2012. Collaborative calibration and sensor placement for mobile sensor networks. In *2012 ACM/IEEE 11th International Conference on Information Processing in Sensor Networks (IPSN)*. IEEE, 73–83.

[18] Y. Yang, Z. Zheng, K. Bian, L. Song, and Z. Han. 2017. Real-time profiling of fine-grained air quality index distribution using UAV sensing. *IEEE Internet of Things Journal* 5, 1 (2017), 186–198.

[19] B. Zhang, T. Xi, X. Gong, and W. Wang. 2019. Mutual information maximization-based collaborative data collection with calibration constraint. *IEEE Access* 7 (2019), 21188–21200.